Notable events

The February 28, 2013, Mw 6.8 South Kamchatka Earthquake

Chebrov et al.

Kamchatka Branch of Geophysical Survey of Russian Academy of Sciences (RAS)

Petropavlovsk-Kamchatsky

1

Notable Events

1.1 The February 28, 2013, Mw 6.8 South Kamchatka Earthquake

V. N. Chebrov[1] (1949-2016), D. V. Chebrov[1], I. R. Abubakirov[1], A. Yu. Chebrova[1], A. A. Gusev[1&2], E. M. Guseva[1], D. V. Droznin[1], S. Ya. Droznina[1], E. M. Ivanova[1], N. M. Kravchenko[1], Yu. A. Kugaenko[1], A. V. Lander[3], E. A. Matveenko[1], S. V. Mitushkina[1], D. A. Ototiuk[1], V. M. Pavlov[1], A. A. Raevskaya[1], V. A. Saltykov[1], A. A. Skorkina[1], N. N. Titkov[1]

Viktor N. Chebrov (1949-2016)

Danila V. Chebrov

1. Kamchatka Branch of Geophysical Survey of Russian Academy of Sciences (RAS), Petropavlovsk-Kamchatsky

2. Institute of Volcanology and Seismology, RAS, Petropavlovsk-Kamchatsky

3. Institute of Earthquake Prediction Theory and Mathematical Geophysics of RAS, Moscow

1.1.1 Introduction

On February 28, 2013, at 14:05 (UTC) a magnitude Mw 6.8 earthquake occurred near the South-East Coast of Kamchatka (Figure 1.1). The source is located in the Pacific Ocean, 120 km east of Severo-Kurilsk, and 270 km south of Petropavlovsk-Kamchatsky. Hypocenter parameters of the earthquake, its strong aftershocks with $ML > 6.0$ and strong earthquakes ($ML > 6.0$) of this area from 1962 to the main event of February 28, 2013 and their magnitude estimations according to several seismological agencies of Russia and the world are given in Table 1.1. According to the Kamchatka Branch of the Geophysical Survey of Russian Academy of Sciences (GS RAS) the earthquake intensities were reported to be up
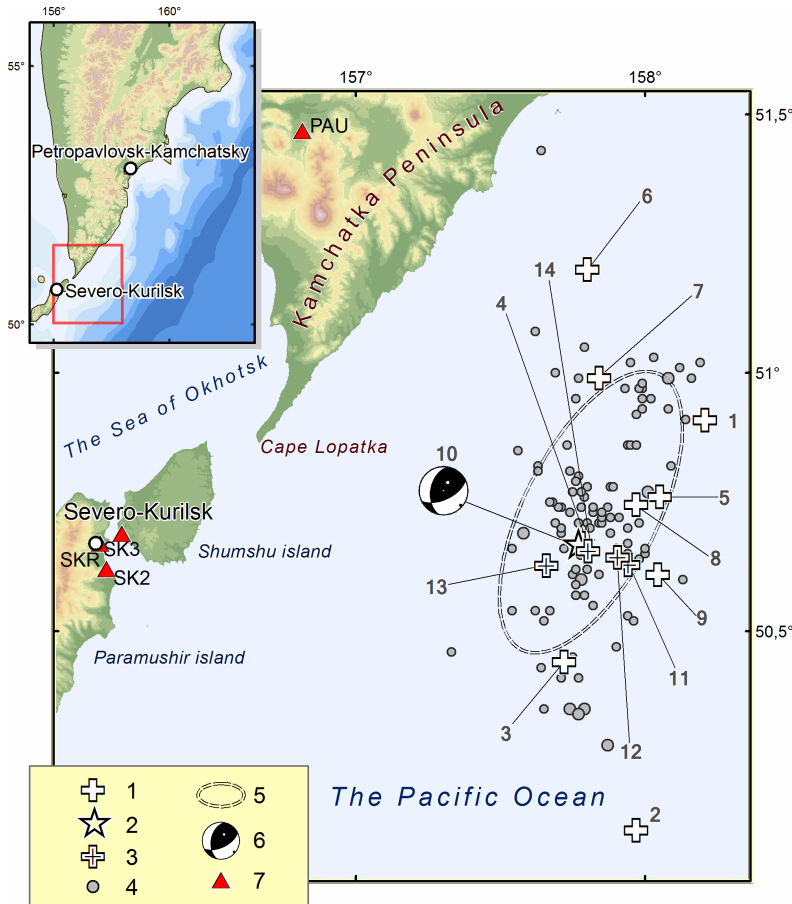
Figure 1.1: *Location scheme for epicenters of the February 28, 2013 earthquake, its aftershocks with ML > 3.5, and strong earthquakes (ML > 6.0) of this region for the period from 1962 to February 28, 2013, according to the catalogue of Kamchatka and the Commander Islands earthquakes (ML > 3.5 corresponds to the catalogue completeness threshold for the Kamchatka regional network within area of responsibility). 1 - epicenters of strong earthquakes of this region for the period from 1962 to February 28, 2013; 2 - the epicenter of the February 28, 2013 earthquake; 3 - epicenters of strong aftershocks (ML > 6.0); 4 - epicenters of aftershocks with 3.5 ≤ ML ≤ 6.0; 5 - 2σ-ellipse approximation of the aftershock zone; 6 - stereogram of the focal mechanism by Global CMT for the main earthquake; 7 - seismic stations. Numeration of earthquakes corresponds to Table 1.1.*

to V-VI on the Medvedev-Sponheuer-Karnik scale (MSK-64) (*Medvedev et al.*, 1965) in settlements on Kamchatka peninsula.

Real-time earthquake processing by Seismological Subsystem of Tsunami Warning System (SS TWS by KB GS RAS) was performed in accordance with accepted time limits. Earthquake alerts and hypocenter parameters were released three times, in 1, 4 and 6 minutes from the first arrival at the closest seismic station. The final SS TWS solution was: 14:05:50 (UTC); 50.89°N, 157.55°E, depth h=61 km, M_S=6.4, M_S(20R)=6.6, ML=6.9. Tsunami alert was not issued. There were no tsunami waves registered by mareographs of Kamchatka Tsunami Warning Center of Roshydromet (Petropavlovsk-Kamchatsky).

The 65 strongest earthquakes final solutions have been published with a delay of no more than a day. In total, during the first 10 days there were 102 aftershocks registered with a magnitude of ML=2.6–6.8. Final processing of the event sequence for the first 10 days was completed by March 10. Further events were processed in the normal mode with a delay of no more than a day.

1.1.2 Focal mechanism of the earthquake

Table 1.2 shows parameters and stereograms of focal mechanisms for the February 28, 2013 earthquake and its strongest aftershocks mentioned in Table 1.1 according to catalogues of Global CMT and KB GS RAS. (Estimates from KB GS RUS are determined by using the polarity of P wave onsets at regional stations). All the mechanisms are consistent with the tectonic condition of sub-horizontal compression in the NW-SE direction. For most mechanisms the flat plane dips under the Kamchatka peninsula,

№	Date YYYY.MM DD.	Time hh:mm:ss	$\phi°$,N	$\lambda°$,E	h, km	K^{F68}	ML	M_c	M_W	m_b	M_S	M_W	m_b	M_S
						KB GS RAS			Global CMT	NEIC(USGS)			Obninsk	
	Hypocenter					Energy class / Magnitudes								

№	Date YYYY.MM DD.	Time hh:mm:ss	$\phi°$,N	$\lambda°$,E	h, km	KB GS RAS K^{F68}	ML	M_c	Global CMT M_W	NEIC(USGS) m_b	M_S	M_W	Obninsk m_b	M_S
				Strong earthquakes of this area for the period from 1962 to February 28, 2013										
1	1966.04.08	01:46:43.4	50.91	158.21	18	13.9	6.2	-	-	6.0	-	-	-	-
2	1966.06.21	23:06:29.2	50.12	157.97	25	13.5	6.0	-	-	5.5	-	-	$M=5$	
3	1973.03.12	19:39:19.6	50.44	157.72	39	14.3	6.4	-	-	6.1	-	-	6.0	6.2
4	1973.04.12	13:49:14.2	50.67	157.78	20	14.2	6.4	-	-	6.1	-	-	6.1	6.4
5	1992.07.13	15:34:03.3	50.76	158.05	39	13.7	6.1	-	6.1	5.7	5.8	6.2	5.8	5.9
6	1993.06.08	13:03:37.0	51.20	157.80	40	15.0	6.8	7.3	7.5	6.4	7.3	7.1	6.5	7.4
7	1999.09.18	21:28:34.2	50.99	157.84	40	13.8	6.2	6.0	6.0	5.9	5.6	6.0	6.2	5.6
8	2006.08.24	21:50:34.1	50.75	157.97	38	14.3	6.4	6.4	6.5	5.9	6.2	6.5	6.0	6.3
9	2008.07.24	01:43:15.8	50.61	158.04	40	13.8	6.2	6.1	6.2	6.0	6.0	6.2	6.1	6.1
				The February 28, 2013 earthquake and its strong aftershocks										
10	2013.02.28	14:05:48	50.672	157.773	61	15.2	6.9	6.6	6.8	6.4	6.7	6.9	6.3	6.8
11	2013.03.01	12:53:49	50.628	157.941	52	14.2	6.4	5.9	6.4	5.7	5.8	6.4	5.8	6.4
12	2013.03.01	13:20:48	50.643	157.904	62	15.1	6.8	6.5	6.5	6.3	6.3	6.5	6.2	6.6
13	2013.03.04	20:56:33	50.627	157.658	51	13.6	6.1	5.1	5.3	5.3	4.8	0	5.4	4.7
14	2013.03.09	14:56:27	50.655	157.803	49	13.7	6.1	5.6	5.8	5.7	5.3	5.8	5.7	5.5

Note: K^{F68} - K-class magnitude of S-wave; ML - local magnitude; M_c - coda magnitude; M_W - moment magnitude; m_b - short-period body-wave magnitude; M_S - surface-wave magnitude.

Table 1.1: *Parameters of strong earthquakes in the South Kamchatka region from 1962 to March 2013, including February 28, 2013 earthquake and its strongest aftershocks.*

which corresponds to the geometry of the subduction zone.

1.1.3 Main features of the aftershocks process

The aftershock sequence of the February 28, 2013 earthquake (Mw=6.8) was selected from the preliminary catalogue using a method after *Molchan and Dmitrieva* (1991); the software was developed by V. B. Smirnov (Lomonosov Moscow State University). This data collection includes 254 earthquakes with magnitudes in the range of ML=2.2–6.8 where ML is calculated from K^{F68} as $ML = K^{F68}/2 - 0.75$, where K^{F68} is the K-class magnitude (*Fedotov*, 1972; *Bormann*, 2002). The cumulative frequency-magnitude plot (Figure 1.2) indicates a catalogue completeness threshold of ML_{min}=3.3 which corresponds to the left edge of the linear part of the plot. Based on this threshold 121 out of 254 earthquakes were obtained from the preliminary catalogue until the end of 2013 for further analysis.

In Figure 1.1 aftershocks are contoured by the dispersion ellipse containing 90% of the aftershocks for the first month after the main earthquake, allowing to estimate the size of the rupture area of the February 28, 2013 earthquake (Mw=6.8) as 90 km (length) × 40 km (width).

The frequency-magnitude plot shows a gap of $\Delta M = 1.3$ between the largest aftershocks and the rest of the sequence (Figure 1.2). Such gaps can be observed between a main shock and the aftershocks. However, in this study the gap is observed between the group of the five strongest events (earthquakes with magnitudes $ML \geq 6.1$, including the main event and 4 strongest aftershocks) and the remaining aftershocks sequence with magnitudes $ML \leq 4.8$. The only earthquake in the magnitude range of ML=4.8–6.0 occurred a month after the main event when the seismic process probably came out of the active phase. Thus, the observed sequence of earthquakes has features of both a swarm and an aftershock sequence with $ML \leq 4.8$.

Figure 1.3 shows the cumulative number of aftershocks over time in log-log scale.

№	Date YYYY.MM .DD	Time hh:mm:ss	h, km	The axes of the principal stresses						Nodal planes						Agency	
				T		N		P		NP1			NP2				
				pl	azm	pl	azm	pl	azm	stk	dip	slip	stk	dip	slip		
10	2013.02.28	14:05:59	45	77	313	2	215	13	124	36	58	92	212	32	86	Global CMT	
		14:05:48	61	59	27	30	225	8	131	65	59	126	191	46	46	KB GS RAS	
11	2013.03.01	12:53:58	44	78	300	0	30	12	120	30	57	90	210	33	90	Global CMT	
		12:53:49	52	62	327	9	221	27	126	43	72	99	196	20	64	KB GS RAS	
12	2013.03.01	13:20:55	41	77	313	2	216	13	126	214	32	87	37	58	92	Global CMT	
		13:20:48	62	66	71	16	201	17	296	193	64	73	49	31	122	KB GS RAS	
13	2013.03.04	20:56:36	44	78	297	1	33	12	124	32	57	88	216	33	93	Global CMT	
		20:56:33	51	79	267	6	32	9	123	27	54	82	221	37	101	KB GS RAS	
14	2013.03.09	14:56:32	47	79	330	3	323	11	132	45	56	94	218	34	84	Global CMT	
		14:56:27	49	81	229	9	49	0	139	41	46	78	238	46	102	KB GS RAS	

Table 1.2: *Parameters of focal mechanisms of the main earthquake and its aftershocks with $ML \geq 6.0$ from Table 1.1 according to the Global CMT and KB GS RAS data.*

Until the end of day 1 the trend is linear thus following Omori's Law with a decay exponent p=1. However, after two earthquakes on March 01, 2013 with Mw=6.4 and Mw=6.5, the behaviour of the sequence changes dramatically, indicating new aftershock process initiated by these two earthquakes. In more detail, the following characteristic stages (Figure 1.3) can be distinguished:

1. Hyperbolic (standard Omori) stage with

$$\frac{dN}{dt} \sim \frac{1}{t}, \tag{1.1}$$

   where N is the cumulative number of aftershocks and t is time, until the strongest aftershocks occur on March 01, 2013. The duration of this stage is ∼23 hours. In this stage, the catalogue completeness threshold is equal to $ML = 3.3$;

2. Strongest aftershocks occur on March 01, 2013 with Mw=6.4 and Mw=6.5; these are accompanied by decaying aftershocks following Omori's law

$$\frac{dN}{dt} \sim \frac{1}{t^p} \tag{1.2}$$

   with $p = 0.7$. The duration of this stage is ∼33 hours. The catalogue completeness of the mode is equal ML=3.3, except for the first 40 minutes;
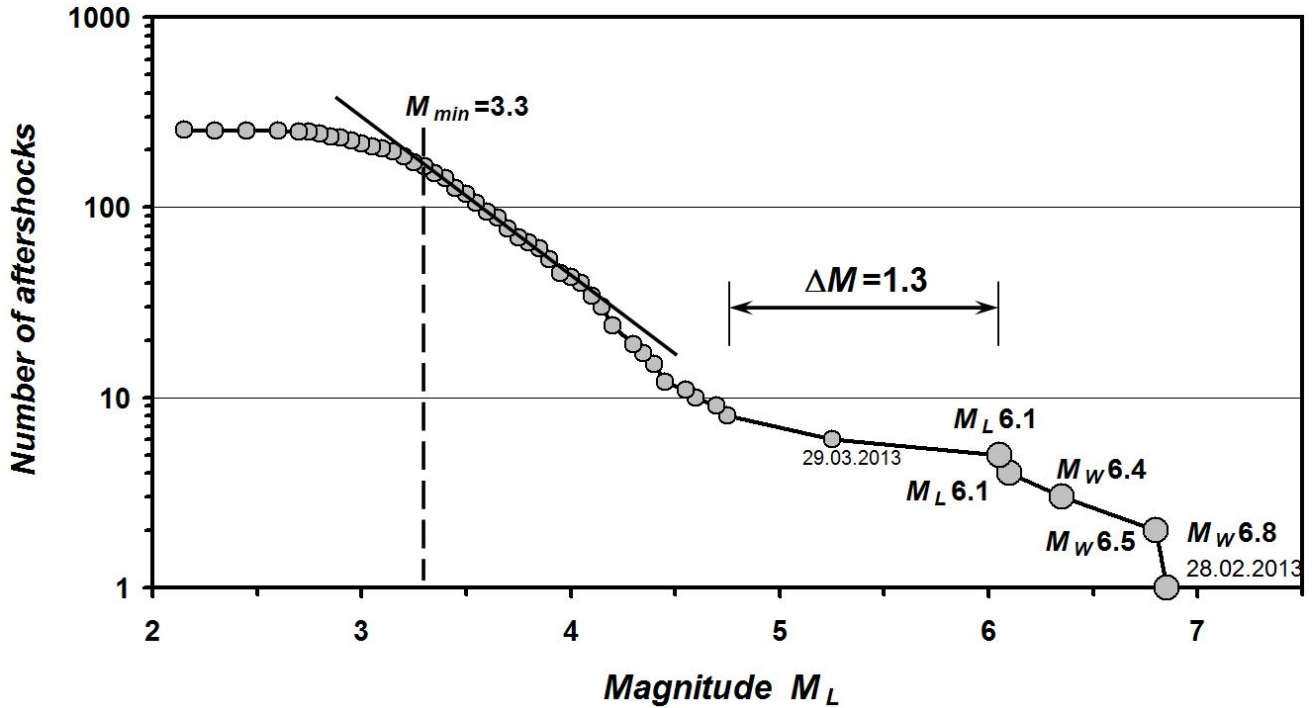
Figure 1.2: *Cumulative frequency-magnitude plot for the aftershocks sequence of the February 28, 2013 earthquake (Mw = 6.8).*

3. The next stage showing a regular hyperbolic-law aftershock decay is the longest one, and lasts until June 2013. This date can be regarded as the end of the aftershock process that began with the earthquake on February 28, 2013, Mw = 6.8; therefore total duration of the aftershock sequence can be estimated as ~100 days. After this date, events in the area in question occur with intervals longer than one month.

1.1.4 Macroseismic data

Macroseismic information is collected for the 46 settlements of the Kamchatka region and the Northern Kuriles based on 109 reports of various sources. For the first time residents of the Kamchatka peninsula actively used an online questionnaire, which can be found on the official website of KB GS RAS (http://www.emsd.ru/lsopool/poll.php). 59 respondents shared their experience from 9 locations. Although the earthquake occurred late at night on March 01, 2013 at 02:05 local time the online questionnaire system immediately began to receive reports from the respondents. By the beginning of the next working day the database of KB GS RAS already collected preliminary information about the intensity of ground shaking in 4 places: Petropavlovsk-Kamchatsky, Viluchinsk, Elizovo and Paratunka.

The earthquake was felt with intensities up to V-VI on the MSK-64 scale in 34 settlements located at epicentral distances from 82 to 492 km. The area of macroseismic effects is about 56,000 km^2. A list of locations with epicentral distance, macroseismic intensity and effects description is given in *Chebrov* (2014).

Figure 1.4 shows a map of isoseismals and reported intensities for the earthquake. Isoseismals are drawn schematically because of the small amount of data due to the lack of settlements in the study area.
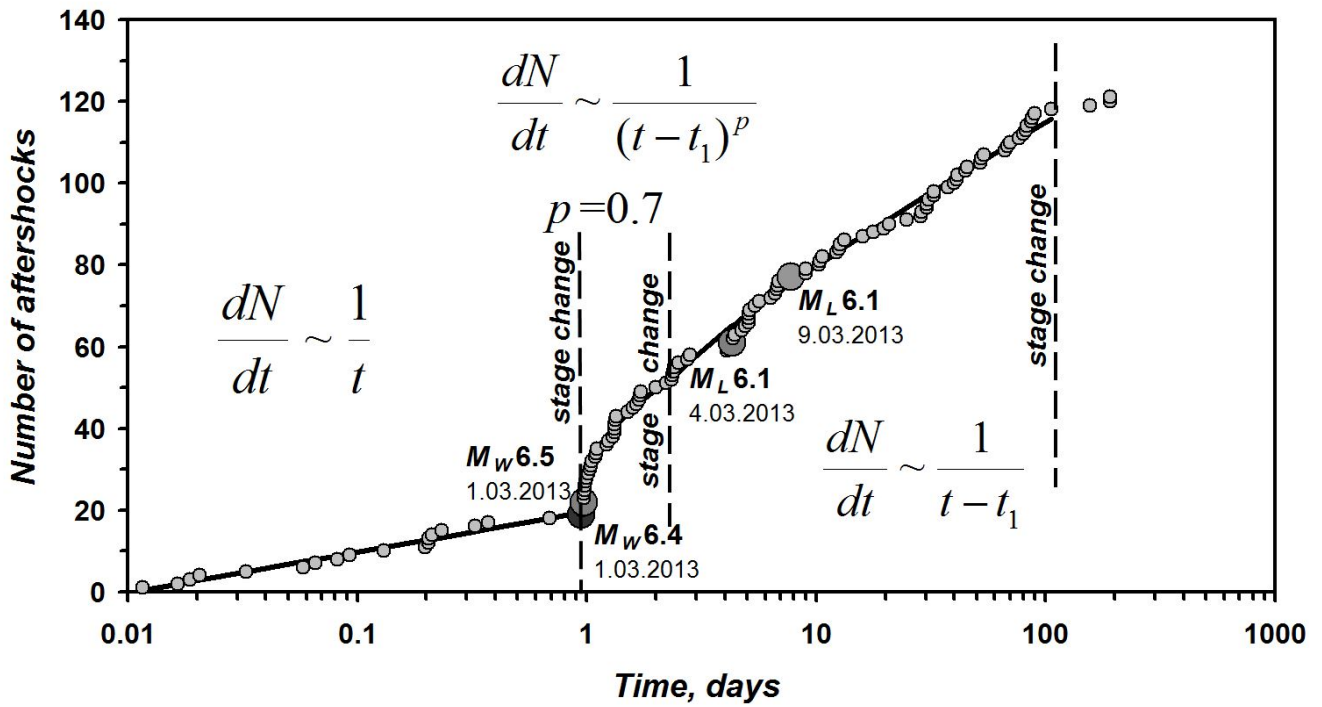
Figure 1.3: *Development of the aftershock sequence with time. Origin time of the plot is set at the moment of the main shock on February 28, 2013 with Mw = 6.8, plus 0.01 day. The cumulative number of aftershocks is shown. The strongest earthquakes of the series are indicated.*
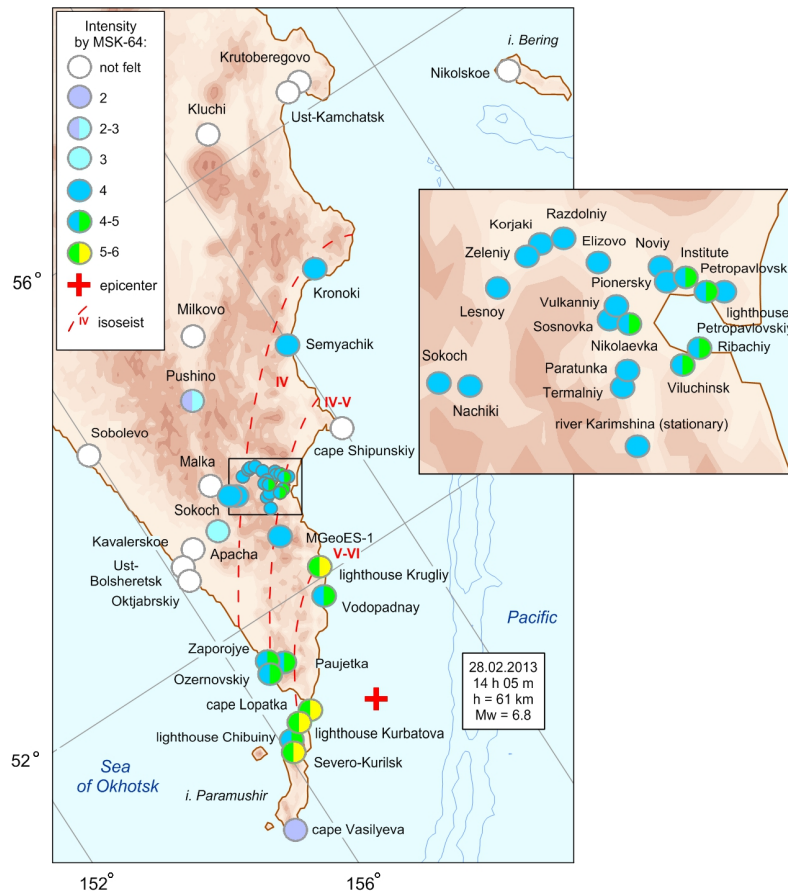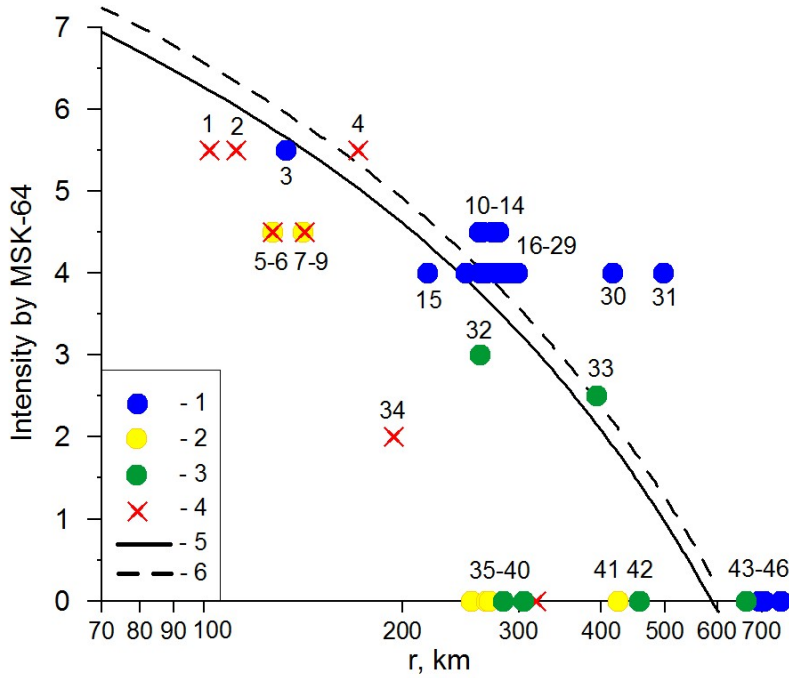

Figure 1.4: *Macroseismic intensity distribution of the February 28, 2013 earthquake.*

Figure 1.5: *Intensity (I) decay with hypocentral distance (r). 1 - observation sites located at the east coast of the Kamchatka Peninsula and Paramushir island; 2 - sites at the west coast; 3 - sites in central Kamchatka; 4 - sites with seismic intensity estimation from transmitted radiogram without text description (lighthouses and the Vodopadnaya meteorological station); 5, 6 - intensity decay curves calculated for Mw = 6.6 and 6.8, respectively, with Equation (1.3).*

Isoseismals are elongated along the east coast of Kamchatka; this pattern is typical for Kamchatka earthquakes.

Figure 1.5 shows the reported intensities over hypocentral distance, I(r), and theoretical decay curves of macroseismic intensity, calculated using the equation after *Fedotov and Shumilina* (1971):

$$I = 1.5 \cdot M - 2.63 \cdot lg(r) - 0.0087 \cdot r + 2.5, \tag{1.3}$$

where I - macroseismic intensity; r - hypocentral distance; M - magnitude (In our calculations we used Mw).

The macroseismic magnitude was estimated as $M = 6.6$; this value was chosen as providing the best fit between intensity decay and observed data. In this fitting, the macroseismic earthquake hypocenter was assumed to coincide with the instrumental one. The graph shows that at equal distances from the hypocenter seismic intensity values in the settlements of the east coast are higher than values in central Kamchatka and the western coast where the earthquake was not felt at distances over 260 km. It should be noted that there is a lack of reported effects at Cape Shipunskiy (Figure 1.4), located on the east coast. Strong winds and storms often mask macroseismic effects at this site. Seismic intensities at the Vodopadnay meteorological station, Chibuiny lighthouses, and Cape Vasilyeva are significantly lower than expected. This may be related to local site conditions, or due to a human bias of intensity values based on the reports of very small staff at the lighthouse.

After the February 28, 2013 earthquake four aftershocks with $ML > 6.0$ (Table 1.1) occurred during the first 9 days and could be felt in Kamchatka (Figure 1.6). All events, including the main one, have a similar pattern in isoseismal maps: the macroseismic effect is higher on the eastern coast of Kamchatka with the strongest shaking recorded at Severo-Kurilsk on the Paramushir island (Figure 1.6).
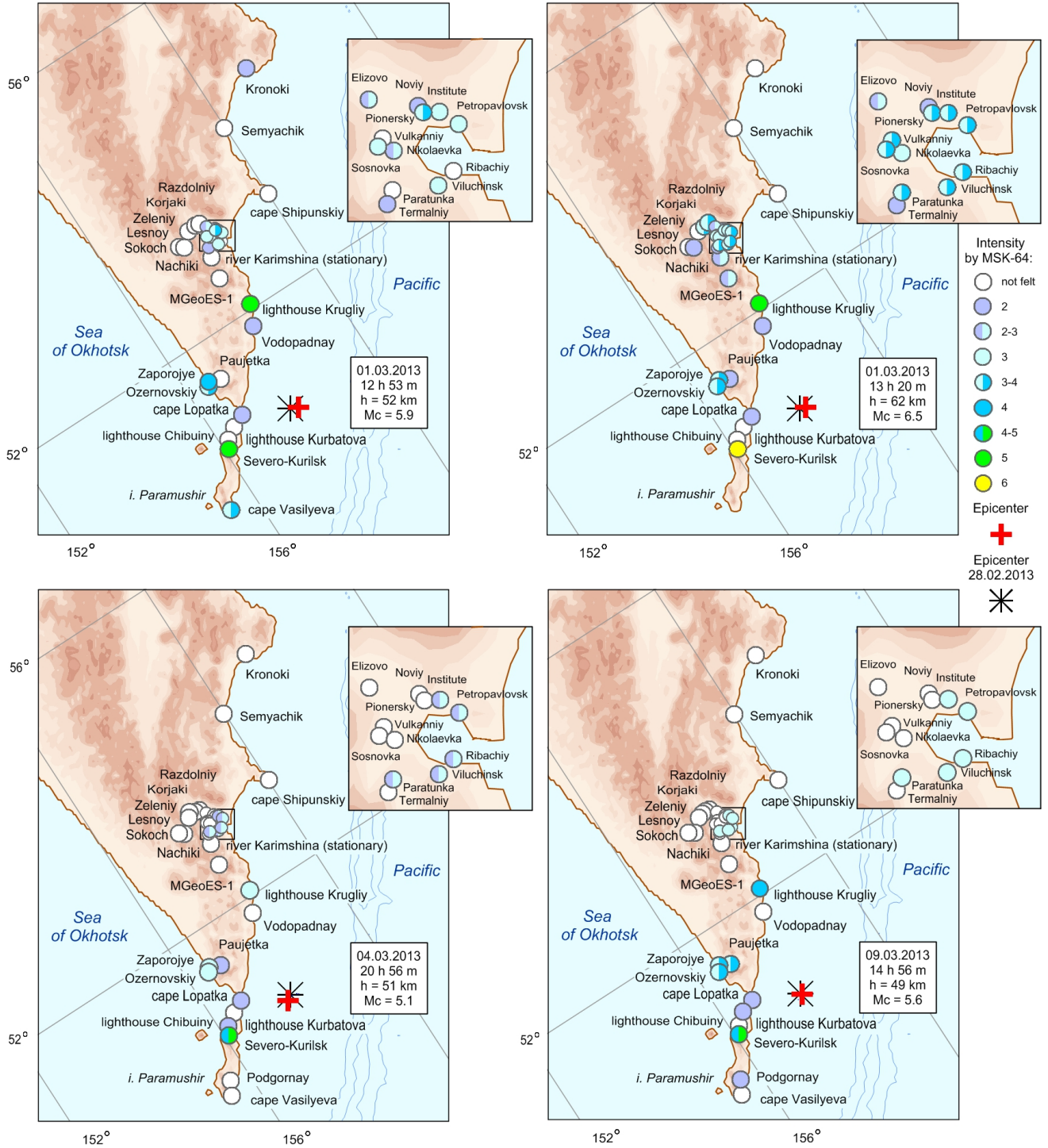
Figure 1.6: *Macroseismic effects of aftershocks of the February 28, 2013 earthquake, see also Table 1.1.*

1.1.5 Ground motion

Figure 1.7 illustrates the records of ground motion at the Severo-Kurilsk seismic station. Peak amplitudes for 29 stations are presented on Figure 1.8 (accelerations) and Figure 1.9 (velocities). When both accelerometer and velocimeter are present at a station, results recovered from records of both instruments are plotted.

There are sometimes significant discrepancies between the estimates of the amplitudes from an accelerometer and a velocimeter. This fact can result from various factors. At some stations the accelerometer is installed on a pedestal, usually in a building (single-storey), while the velocimeter is installed outside the building, at distances of ≈40 m, in a borehole at depths of 5-30 m. Additionally, instrument orientation azimuths for borehole instruments could bear large errors.

The decay of amplitudes with hypocentral distance r is analysed in the next paragraphs. Figure 1.8 shows the peak acceleration of the vertical and horizontal components with hypocentral distance. For comparison, two peak acceleration decay curves from other sources are plotted. Of the two parallel solid gray lines, the lower one is after *Fukushima and Tanaka* (1990) (with their epicentral distances converted to hypocentral ones). It follows the trend

$$A \sim r^{-1.218} \tag{1.4}$$

Its intersection with the y-axis corresponds to Mw = 7.0. The upper line is plotted through an anchor point at r = 200 km using a point estimate derived from empirical scaling after *Gusev et al.* (1997). In that paper, only epicentral distances between 50-200 km were considered. Therefore, the line was plotted through the anchor point with the slope identical to that of *Fukushima and Tanaka* (1990). None of these approximations is acceptable. At distances above 300 km data points are below both straight lines. An alternative linear approximation of the data was found, based on the least squares method (dot-dashed line), with a slope of -2.55. Despite some improvement of the fit, the general agreement was still poor. As a final approximation we prefer three-segment broken line (dashes), with corner points at r = 300 and 600 km, and slopes that vary, from left to right, from -1.37 to -2.42 and to -5.8.

In Figure 1.9, peak velocities are depicted. The reference straight line represents the calibration curve of the local K-class magnitude scale K^{F68} (*Fedotov*, 1972) with the standard slope of -1.75, and with its position along the y-axis selected for the best fit. This selection gives the corresponding magnitude value $K^{F68} = 16.3$. The peak velocity was estimated as 2π (A/T) where A/T is the standard input of K^{F68} magnitude calculation. The actual value of K^{F68} for the main shock is 15.3, indicating amplitudes about 3.2 times lower than expected from the above estimate of K^{F68}=16.3. The discrepancy appears to be associated with significantly broader bandwidth of the digital velocimeter as compared to the emulated band-limited signal of 1.2s VEGIK seismograph channel used for the K^{F68} calculation. The qualitative agreement of the trend for observed data with the trend of the calibration curve is quite acceptable. It should be noted that the original calibration curve was constructed up to the 600 km distance; the success of its extrapolation up to 1600 km was unexpected.

A more detailed analysis of amplitudes can be carried out after careful classification of stations by their soil types. According to the analysis of limited data for amplitudes of the February 28, 2013 earthquake,
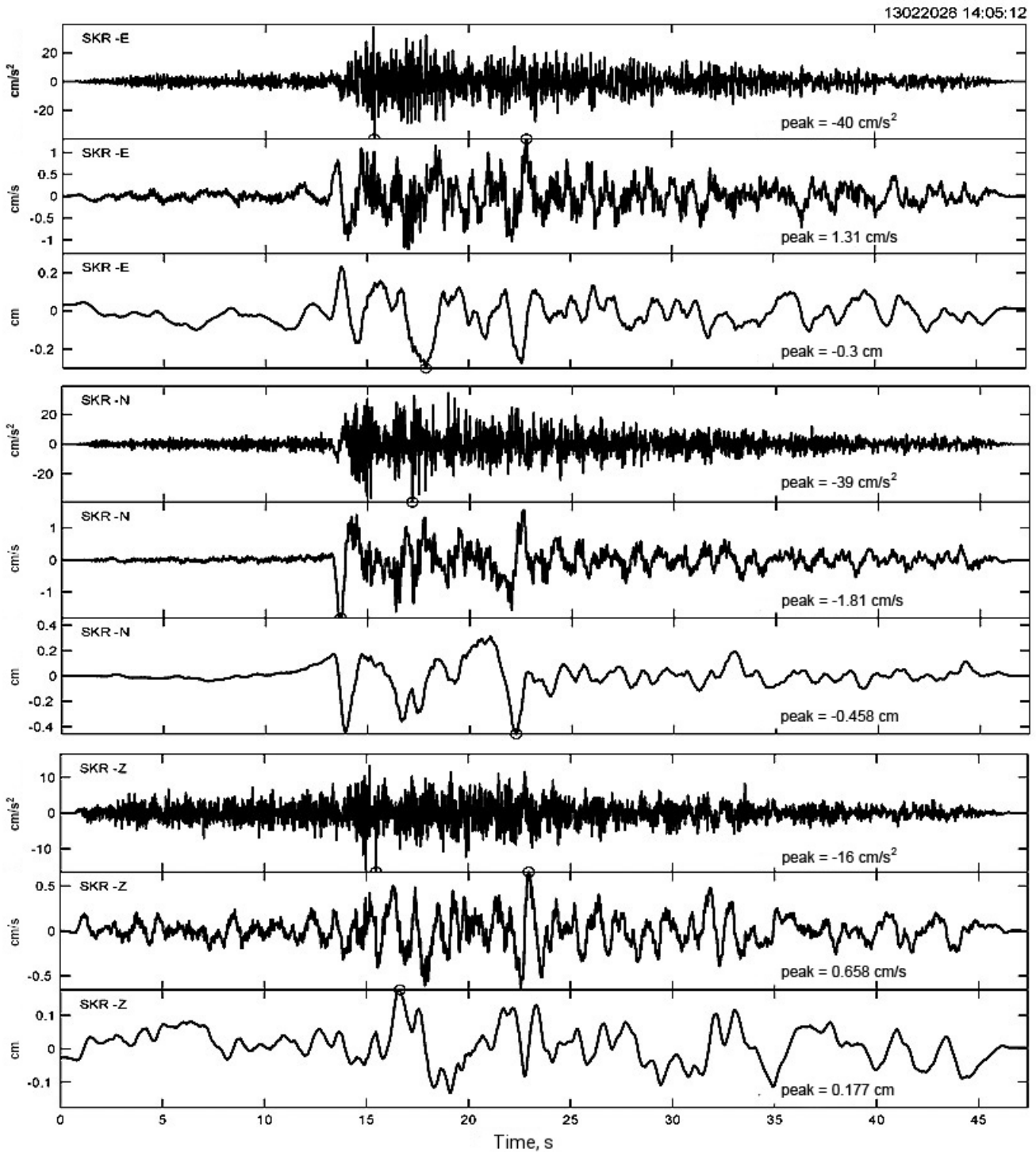
Figure 1.7: *Example of acceleration records at channels of digital Guralp CMG-5 accelerograph with the GEOSIG recorder at Severo-Kurilsk station (SKR), one of the closest to the epicenter, and recovered signals of velocity and displacement from these records in the frequency range from 0.1 to 40 Hz.*
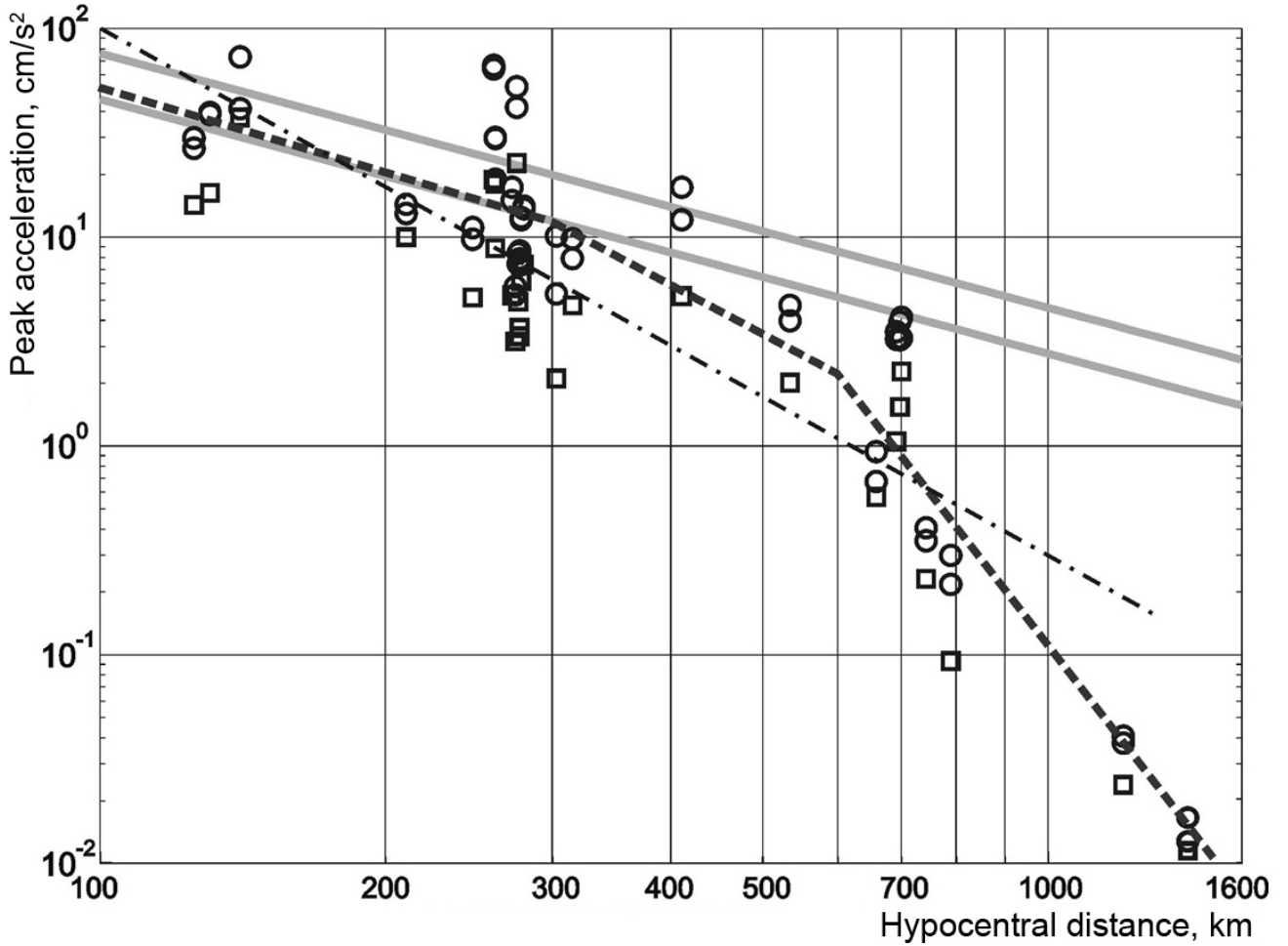
Figure 1.8: *Peak acceleration with hypocentral distance. Circles and squares correspond to acceleration values on the horizontal and vertical components, respectively. Gray lines follow decay approximations based on Fukushima and Tanaka (1990) (lower) and Gusev et al. (1997) (top), for details see the text. Dot-dashed line shows a linear approximation of the data, which is not acceptable. The dashed line is the accepted 3-segment approximation.*

preliminary conclusions can be made:

(1) the level of acceleration and velocity amplitudes for the earthquake is approximately consistent with average tendencies for Kamchatka;

(2) the distance decay for peak accelerations over the 100-300 km range is comparable to that for earthquakes of Kamchatka and Japan. The trend of $A \sim r^{-1.218}$ is consistent with the data. At larger distances, the decay becomes much steeper.

(3) the distance decay for peak velocities in the entire investigated distance range of 100-1600 km matches the calibration curve for regional K-class magnitude, K^{F68}, with its trend $V \sim r^{-1.75}$.

1.1.6 Conclusion

The February 28, 2013 earthquake of Mw = 6.8 is a regular event in the seismic process of the Kuril-Kamchatka subduction zone. The earthquake occurred at the latitude of the Cape Lopatka. This segment of the Kuril-Kamchatka arc is one of the most seismically active areas in the North-West
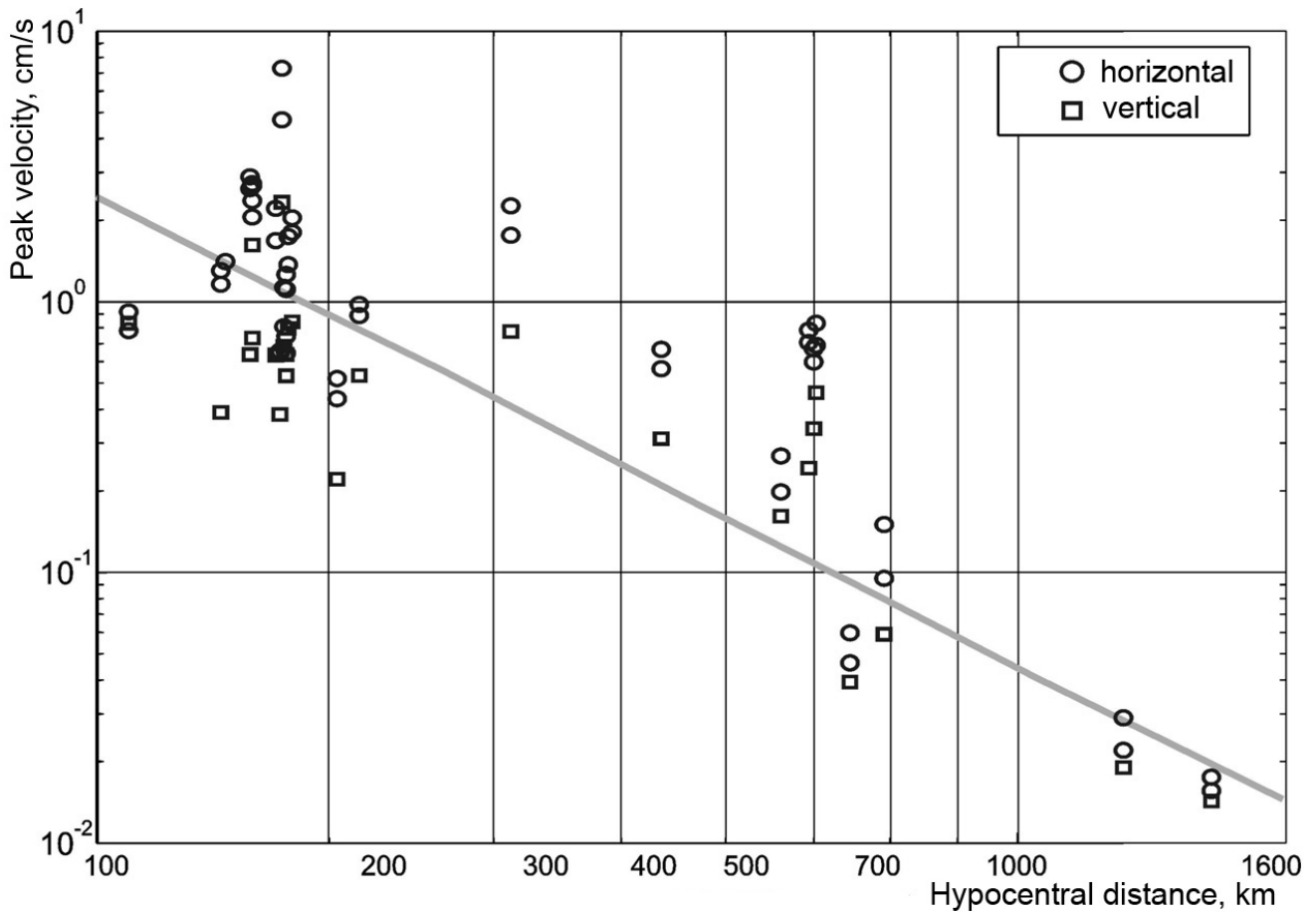
Figure 1.9: *Peak velocities with hypocentral distance. The line shows the calibration curve of the Kamchatka K-class magnitude scale K^{F68} (Fedotov, 1972), with a value of $K^{F68} = 16.3$.*

Pacific. There have been repeatedly earthquakes with $M > 8$ that caused tsunamis and intensities of ground shaking up to IX on the MSK-64 scale in the south of Kamchatka (*Godzikovskaya*, 2010; *Kondorskaya and Shebalin*, 1977).

The last earthquakes with magnitudes of $M \geq 7.0$ were recorded in the area of the North Kuriles in 1955 (on November 23, 1955, $M = 7.3$ (*Kondorskaya and Shebalin*, 1977)) and in 1973 (on February 28, 1973, Mw = 7.4 (*Gusev and Shumilina*, 2004)), and off the coast of south Kamchatka - in 1993 (on June 08, 1993, Mw = 7.5 (*Gusev and Shumilina*, 2004)) and in 1999 (on March 08, 1999, Mw = 6.9). This area is located in an extensive fault zone that was ruptured by the strong catastrophic Kamchatka earthquake on April 11, 1952 with Mw = 9.0 (*Gusev and Shumilina*, 2004), and probably lies in the fault zone of the first historical earthquake in Kamchatka on October 17, 1737 with Mw = 9.2 (*Gusev and Shumilina*, 2004) described by *Krasheninnikov* (1949) and *Godzikovskaya* (2010) as well.

Parameters of the February 28, 2013 earthquake have been evaluated by SS TWS within 6 minutes, what is in accordance with accepted time limits. In urgent mode aftershocks have been processed. Macroseismic data have been collected for the region of Kamchatka and Northern Kuriles.

The actual time-magnitude pattern of the observed earthquake sequence is specific, with its properties between a standard aftershock sequence with a single mainshock, and a typical swarm with no main event. The aftershock cloud approximately covers an area of 90 km (length) × 40 km (width); these

figures provide a maximum estimate for the main shock fault size.

The analysis of peak accelerations shows typical amplitudes and decay within 250 km epicentral distance. At larger distances, a much stronger decay was revealed. The decay of peak amplitudes with epicentral distance matches the average trend for the Kamchatka region well. The February 28, 2013 earthquake of Mw = 6.8 is the first earthquake of such magnitude in the Kamchatka region, that is recorded by the digital new system of seismic observations set by KB GS RAS between 2005 and 2010 (*Chebrov et al.*, 2013).

1.2 References

Bormann, P. (Ed.) (2002): *New Manual of Seismological Observatory Practice (NMSOP)*, IASPEI, GFZ GeoForschungsZentrum Potsdam, Potsdam, Vol. 1-2, DOI:10.2312/GFZ.NMSOP-2.

Chebrov, V. N., D. V. Droznin, Yu. A. Kugaenko, V. I. Levina, S. L. Senyukov, V. A. Sergeev, Yu. V. Shevchenko and V. V. Yashchuk (2013), The system of detailed seismological observations in Kamchatka in 2011, *Journal of Volcanology and Seismology*, *7*(1), 16–36, DOI:10.1134/S0742046313010028.

Chebrov V. N. (Ed.) (2014): *Strong earthquakes of Kamchatka in 2013*. Petropavlovsk-Kamchatsky: New Book Company, 2014. 252 p. ISBN 978-5-87750-298-7 [In Russian].

Fedotov, S. A. (1972), *Energy classification of the Kuril-Kamchatka earthquakes and problem of magnitude determination*, Nauka. 117 p. [in Russian].

Fedotov, S. A. and L. S. Shumilina (1971), Seismic hazard of Kamchatka, *Izv. Akad. Nauk SSSR Fiz. Zemli.*, *9*, 3-15.

Fukushima, Y. and T. Tanaka (1990), A new attenuation relation for peak horizontal acceleration of strong earthquake ground motion in Japan, *Bull. Seismol. Soc. Am.*, *80*(4), 757-783.

Godzikovskaya, A. A. (2010), Macroseismic descriptions and parameters of Kamchatka earthquakes that occurred during the preinstrumental period of observation, *Journal of Volcanology and Seismology*, *4*(5), 354–366, DOI:10.1134/S0742046310050052.

Gusev, A. A., E. I. Gordeev, E. M. Guseva, A. G. Petukhin and V. N. Chebrov (1997), The first version of the Amax (Mw, R) relationship for Kamchatka, *Pure and applied geophysics*, *149*(2), 299–312, DOI:10.1007/s000240050027.

Gusev, A. A. and L. S. Shumilina (2004), Recurrence of Kamchatka strong earthquakes on a scale of moment magnitudes, *Izvestiya Physics of the Solid Earth*, *40*(3), 206-215.

Kondorskaya, N. V. and N. V. Shebalin (1977), New catalog of strong earthquakes in the territory of the USSR from ancient times to 1975, Academy of Sciences, Moscow (English translation, updated through 1977, available as Report SE-31, World Data Center A for Solid Earth Geophysics, NOAA, Boulder, CO, 1982, 606 p.)

Krasheninnikov, S. P. (1949), The description of land Kamchatka, reprinted by the USSR Academy of Sciences Press, Moscow. 840 p. [in Russian].

Medvedev, S. V., V. Shponhoyer and V. Karnik (1965), Scale of seismic intensity MSK-64, *Academy of Science of USSR*, 11.

Molchan, G. M. and O. E. Dmitrieva (1991), Identification of aftershocks: review and new approaches, *Computational Seismology*, *24*, 19–50.